

A peer-reviewed version of this preprint was published in PeerJ on 10 December 2015.

[View the peer-reviewed version](https://doi.org/10.7717/peerj.1491) (peerj.com/articles/1491), which is the preferred citable publication unless you specifically need to cite this preprint.

Hisakawa N, Quistad SD, Hester ER, Martynova D, Maughan H, Sala E, Gavrilov MV, Rohwer F. 2015. Metagenomic and satellite analyses of red snow in the Russian Arctic. PeerJ 3:e1491
<https://doi.org/10.7717/peerj.1491>

Metagenomic and satellite analyses of red snow in the Russian Arctic

Nao Hisakawa, Steven Quistad, Eric Hester, Daria Martynova, Heather Maughan, Enric Sala, Maria Gavrilov, Forest Rohwer

Cryophilic algae thrive in liquid water within snow and ice in alpine and polar regions worldwide. Blooms of these algae lowers albedo (reflection of sunlight), thereby altering melting patterns (Kohshima et al. 1993; Lutz et al. 2014; Thomas & Duval 1995) . Here metagenomic DNA analysis and satellite imaging were used to investigate red snow in Franz Josef Land in the Russian Arctic. Franz Josef Land red snow metagenomes confirmed that the communities are composed of the autotroph *Chlamydomonas nivalis* that is supporting a complex viral and heterotrophic bacterial community. Comparisons with white snow communities from other sites suggest that snow and ice are initially colonized by fungal-dominated communities and then succeeded by the more complex *C. nivalis*-heterotroph red snow. Satellite image analysis showed that red snow covers up to 80% of the surface of snow and ice fields in Franz Josef Land and globally. Together these results show that *C. nivalis* supports a local food web that is on the rise as temperatures warm, with potential widespread impacts on alpine and polar environments worldwide.

Metagenomic and Satellite Analyses of Red Snow in the Russian Arctic

Naoh Hisakawa¹, Steven Quistad¹, Eric Hester¹, Daria Martynova^{2,3}, Heather Maughan^{4*}, Enric Sala⁵, Maria Gavrilov³, Forest Rohwer¹

¹Department of Biology, San Diego State University, 5500 Campanile Drive, San Diego, CA 92182

1 ²White Sea Biological Station, Zoological Institute, Russian Academy of Sciences,
2 Universitetskaya nab. 1, 199034, St. Petersburg, Russia

3 ³National Park “Russian Arctic”, pr. Sovetskikh Kosmonavtov, 57, Arkhangelsk, Arkhangelsk
4 Oblast, 163000, Russia

5 ⁴Ronin Institute, Montclair, NJ 07043 USA

6 ⁵National Geographic Society, Washington, DC 20036

7

8

***Corresponding author:** Heather Maughan, 296 Concession 6E, RR3, Mildmay, ON N0G 2J0
Canada, heathermaughan@gmail.com

Keywords: red snow, snow, watermelon snow, Franz Josef Land, arctic, metagenomics, viruses, phage

9 **Abstract**

10 Cryophilic algae thrive in liquid water within snow and ice in alpine and polar regions
11 worldwide. Blooms of these algae lowers albedo (reflection of sunlight), thereby altering melting
12 patterns (Kohshima et al. 1993; Lutz et al. 2014; Thomas & Duval 1995). Here metagenomic
13 DNA analysis and satellite imaging were used to investigate red snow in Franz Josef Land in the
14 Russian Arctic. Franz Josef Land red snow metagenomes confirmed that the communities are
15 composed of the autotroph *Chlamydomonas nivalis* that is supporting a complex viral and
16 heterotrophic bacterial community. Comparisons with white snow communities from other sites
17 suggest that snow and ice are initially colonized by fungal-dominated communities and then
18 succeeded by the more complex *C. nivalis*-heterotroph red snow. Satellite image analysis showed
19 that red snow covers up to 80% of the surface of snow and ice fields in Franz Josef Land and
20 globally. Together these results show that *C. nivalis* supports a local food web that is on the rise
21 as temperatures warm, with potential widespread impacts on alpine and polar environments
22 worldwide.
23

24 **Introduction**

25 *Chlamydomonas nivalis* is a unicellular snow alga that has been detected worldwide within the
26 upper snow layer in polar and alpine regions (Guiry et al. 2014) and is especially abundant in the
27 Arctic pack ice (Gradinger & Nurnberg 1996). In these harsh environments, *C. nivalis* has
28 adapted to intense UV exposure by producing astaxanthin, a UV-screening pigment that
29 produces a visible red hue in snow (Gorton & Vogelmann 2003; Williams et al. 2003). *C. nivalis*
30 spends most of its growth season in its red colored stage (Gorton & Vogelmann 2003; Stibal et
31 al. 2007; Williams et al. 2003); this coloration is visible across the snow/ice surface and can
32 reduce albedo to 40% [c.f., fresh snow albedo of 75% (Thomas & Duval 1995)]. The lower
33 albedo increases local temperature, promoting snow and ice melting and increasing the
34 abundance of *C. nivalis* (Thomas & Duval 1995). Through this positive feedback loop the
35 abundance of *C. nivalis* amplifies snow and ice melting. *C. nivalis* may also contribute to CO₂ by
36 fixing carbon. However, if there is a red snow associated heterotrophic viral and microbial
37 community, much of this newly fixed carbon may be released via respiration (Bardgett et al.

38 2008). *C. nivalis*-produced dissolved organic carbon (DOC) could also contribute to priming
39 when the melt water washes into the ocean (Geller 1986; Hamer & Marschner 2002; Madigan et
40 al. 1997; van Nugteren et al. 2009) and lead to increased CO₂ release.

41

42 **Materials and Methods**

43 *Analysis of satellite images:* Remote sensing methods were used to estimate abundances
44 of red snow at eleven locations around the world (see Supplementary Materials). Landsat
45 satellite images were acquired from the USGS Earth Explorer site
46 (<http://earthexplorer.usgs.gov/>) and image analysis methods were adapted from Takeuchi et al.
47 (Takeuchi et al. 2006) as described in the Supplementary Materials. Red to green reflectance
48 band ratios with wavelengths 630 – 690 nanometers and 520 – 600 nanometers, respectively,
49 were used to detect red snow in the satellite images. The spectral reflectance of red snow shows
50 that it has higher reflectance in the red band than in the green band, while the spectral reflectance
51 of snow and ice has higher reflectance in the green band than the red band (Takeuchi et al. 2006).
52 Therefore, red to green reflectance band ratios that are less than 1.0 are more likely to signify
53 white snow or ice while band ratios that are greater than 1.0 are more likely to signify red snow
54 or ice.

55 ArcGIS version 10.2 was used to calculate the reflectance band ratios. Previous research
56 indicates areas with reflectance band ratios > 1.02 are bright red when observed in the field
57 (Takeuchi et al. 2006). For this analysis, areas with reflectance band ratios greater than 1.0 were
58 considered to have a significant amount of red snow because such values have been shown to
59 have an algal cell volume of 100 ml m⁻² (Takeuchi et al. 2006). Using the positive linear
60 correlation between algal cell volume biomass and reflectance band ratio, it was assumed that the
61 higher the reflectance band ratio, the higher the algal cell volume biomass. With this in mind, the
62 reflectance band ratios were divided into five categories for optimal visualization of various
63 levels of concentrations of red snow (Supplementary Table 1 and Figure 1B).

64 *Algal biomass:* To estimate the algal biomass for each location, the surface area
65 belonging to each reflectance band ratio category was multiplied by the mean algal biomass of
66 that category. Although the extent of the area of interest is the same for all three images, they
67 have varying amounts of surface area where red snow can exist due to shifts in snow and ice
68 coverage. Therefore, in addition to the total algal biomass, the total area of snow coverage and

69 the percentage of the total area of snow that was covered with different abundances of algae
70 were calculated. A pixel was categorized as snow if its normalized difference snow index
71 (NDSI) was greater than 0.4 and, to mask out water, if its near-infrared reflectance value was
72 greater than 0.11 (Sibandze et al. 2014). The number of pixels that meet these conditions was
73 multiplied by the area of the pixel to get the total area of ground covered by snow/ice. To
74 calculate the percentage of the total area of snow that is covered with algae, the total area with
75 each algal abundance level was divided by the total area of snow coverage.

76 *Metagenomic sequencing:* Red snow samples were examined with microscopy to confirm
77 the presence of *C. nivalis* based on morphology (Muller et al. 1998). Three red snow samples of
78 ~15 L were collected, melted, and passed through a 0.22 μm sterivex filter. Total DNA was
79 extracted in the field using the Soil DNA Isolation kit with a custom vacuum manifold (Norgen
80 BioTek Corp., cat# 26560). From the total DNA, a NexteraXT library kit was used to prepare
81 DNA libraries for sequencing on the Illumina MiSeq. The libraries were named Nansen (135,749
82 reads), Greely_1 (86,932 reads) and Greely_2 (47,507 reads). Each metagenome was passed
83 through the following quality control pipeline. PrinSeq was used to quality filter reads below 100
84 bp in length and below an average quality score of 25, and to remove duplicates and sequence
85 tags (Schmieder & Edwards 2011b). Reads assigned as human were removed using DeconSeq
86 (Schmieder & Edwards 2011a). Post quality control, the Nansen library contained 121,455 reads,
87 Greely_1 contained 69,918 reads, and Greely_2 contained 40,344 reads. Seven publicly
88 accessible snow metagenomes from Svalbard glaciers (a.k.a., white snow throughout manuscript)
89 sampled April through June were downloaded from MG-RAST and reads were quality filtered
90 using the same pipeline as the FJL red snow libraries (Maccario et al. 2014). The red snow and
91 white snow libraries were compared to the KEGG database to assign reads to KEGG pathways
92 (e-value < 1×10^{-5} ; >60% identity; >15 aa minimum alignment length). Estimations of taxonomic
93 composition of communities were based on translated comparisons to the non-redundant protein
94 database M5NR (e-value < 1×10^{-5} ; >60% identity; >15 aa minimum alignment length). The
95 dataset was normalized to ensure similar numbers of reads were used for each sample, and then
96 raw read counts were log transformed. Statistical differences between red snow and snow in the
97 numbers of reads assigned to KEGG pathway groups were identified by ANOVA. Multivariate
98 statistics were performed in R using the vegan (Dixon 2003), clustsig and the stats packages. The
99 *adonis* function was used to compare metagenome compositions; *vegdist* was used to generate

100 distance matrices; *simprof* was used to cluster metagenomes based on similarity; and *prcomp*
101 was used to perform Principal Component Analysis.

102

103 **Results and Discussion**

104 *Detection of red snow in a global sample of satellite images:* Satellite images with
105 spectral reflectance data were used to approximate snow and ice cover, as well as red algae
106 abundance (Takeuchi 2009; Takeuchi et al. 2006) over several years in Franz Josef Land, as well
107 as eleven other regions of United States, Canada, Greenland, Norway, Austria, India, and New
108 Zealand (Supplementary Figure 1). Red snow was detected at all eleven locations in all the years
109 (Figure 1A). The total area of snow and ice were lowest in the most recent year (2013, 2014 or
110 2015, depending on the location; Supplementary Figure 2; Greenland was the exception to this
111 trend). At least 50% of the total snow/ice area was covered with algae for the most recent year
112 analyzed (Supplementary Figure 2; exception New Zealand and Franz Josef Land). In seven of
113 the locations, over 80% of the total snow and ice fields were covered in red algae in the most
114 recent year analyzed (Supplementary Figure 2).

115 We performed a walking transect from sea level to the glacier on Nansen Island in Franz
116 Josef Land in August 2013 (to be described in a separate manuscript). Therefore, this region was
117 targeted for more detailed analysis. Around and on Nansen, the total red snow algal biomass
118 increased by 124% from 1986 to 2002 and by 15% from 2002 to 2006, then decreased by 63%
119 from 2006 to 2015 (Figure 1B). These changes in algal cover co-occurred with a total decline in
120 the snow and ice cover (Figure 1B). Visual inspection of the snow and ice on Nansen Island in
121 August of 2013 confirmed the presence of red colored snow and microscopy of red snow
122 samples showed *C. nivalis* cells. Taken together, these results show that even as total snow and
123 ice cover declines, red snow cover is still highly prevalent or increasing both in Franz Josef Land
124 and other alpine/polar regions.

125 *Microbes present in snow and red snow:* For metagenomic sequencing, one and two red
126 snow samples were taken from Nansen and Greeley Islands, respectively. Seven white snow
127 metagenomes from Svalbard glaciers were also downloaded and analyzed for comparison (see
128 Methods & Supplementary Materials). The genus-level taxonomic compositions of white snow
129 and red snow were significantly different (ADONIS; $F = 4.567$; $p = 0.007$). When samples were
130 clustered according to their taxonomical similarities, one red snow sample taken at Greeley Island

131 grouped with a Svalbard glacier sample; otherwise the red snow and white snow samples
132 clustered separately (Supplementary Figure 3). This indicates minimal overlap in microbial
133 composition at the genus level.

134 Community DNA sequences were further compared using multivariate analyses with the
135 top 10 most variable taxa (Supplementary Figure 4). The first two principal components
136 explained 70% of the between-sample variation in microbial community members. The first
137 principal component described red snow as having higher abundances of species from the
138 bacterial genera *Pseudoalteromonas*, *Alteromonas*, *Vibrio*, and *Pedobacter*, whereas white snow
139 had higher abundances of species from the eukaryotic genera *Aspergillus* and *Neurospora*, as
140 well as the bacterial genera *Nostoc*, *Bacillus* and *Spirosoma*. Red snow had greater overall
141 abundances of Bacteria and viruses (Figure 2A) and a lower abundance of Eukaryotes (Figure
142 2A). The bacterial communities associated with red snow have also been observed in an alpine
143 region (Thomas & Duval 1995) and are probably support by photosynthate from the *C. nivalis*.
144 Evidence also suggests that bacterial cells may physically attach to the outer mucilaginous
145 coating of *C. nivalis* in red snow forming an arctic holobiont (Remias et al. 2005; Thomas &
146 Duval 1995).

147 The metagenomes were also used to verify the presence of *Chlamydomonas* in snow
148 samples (Supplementary Figure 5). Of the sequence reads assigned to Eukaryotes, the proportion
149 of reads assigned to the *Chlamydomonas*-containing phylum Chlorophyta was higher in red
150 snow than white snow (Figure 2B). Conversely, the proportion of reads assigned to the fungal
151 phylum Ascomycota was higher in white snow (Figure 2B).

152 *Functional capabilities of microbial communities in red snow and snow:* The
153 metagenomes were also analyzed for potential metabolic functions. The functions encoded by
154 the red and white snow samples clustered into 8 significant groups, with the red snow samples
155 from Greely and Nansen Islands forming a significant cluster (Supplementary Figure 6). Four
156 white snow samples formed a cluster and the remaining snow samples clustered individually.
157 Multivariate analysis of the top 10 most variable functions showed that the first two principal
158 components explained 82% of the variation in the abundances of functional pathways
159 (Supplementary Figure 7). The first component (70% of the variation) showed that the red snow
160 had higher abundances of genes involved in membrane transport, carbohydrate metabolism,
161 nucleotide and amino acid synthesis/degradation, and energy metabolism. White snow

162 communities were shifted toward cell growth and death, folding sorting and degradation,
163 transcription, transport and catabolism pathways and pathways annotated as important in
164 neurodegenerative diseases (i.e., mitochondrial functions in Eukaryotes).

165 In order to examine whether microbial communities in red snow encoded completely
166 different functional capabilities from those in snow, the numbers of reads assigned to all KEGG
167 pathways were compared using a matrix of Bray-Curtis dissimilarities. Overall the abundances
168 of KEGG pathways were not significantly different between red snow and white snow
169 (ADONIS; $F = 2.135$; $p = 0.12$). However, separate analyses that compared individual pathways
170 between red snow and white snow identified several pathways as significantly different,
171 including pathways related to sugar biosynthesis and metabolism and energy metabolism. Red
172 snow communities had higher abundances of genes that encode lipopolysaccharide biosynthesis
173 and peptidoglycan biosynthesis. Red snow also had a higher proportion of reads assigned to
174 oxidative phosphorylation, methane metabolism, carbon fixation in photosynthetic organisms
175 and carbon fixation pathways (Figure 3B). White snow had higher relative abundances of genes
176 that encode glycan biosynthesis and related pathways such as GPI-anchor biosynthesis, other
177 types of O-glycan biosynthesis and various types of N-glycan biosynthesis (Figure 3A). Taken
178 together, these results support the hypothesis that red snow communities include primary
179 producers with a large, heterotrophic community including viruses. In contrast, white snow
180 communities appear to be dominated by fungi, maybe eating refractory organic carbon delivered
181 with the snow (Clarke & Noone 1985; Rosen et al. 1981; Thevenon et al. 2009).

182

183 **Conclusions**

184 Microbiology of snow and ice fields has a long history, including a reference to red snow
185 by Aristotle. However, until now we have not had the tools to determine the full extent and
186 makeup of these communities. Here we use a combination of satellite and metagenomic
187 approaches to show that red snow covers up to 80% of the examined ice and snow fields.

188 Metagenomics of red snow from Franz Josef Land, one of the most remote polar land masses in
189 world, show that these communities support a full food web ranging from algae to heterotrophic
190 microbes to viruses. Because of the reduced albedo associated with these communities, red snow
191 creates a positive feedback loop that increases its abundance while simultaneously melting ice
192 and snow (Figure 4). In addition to the direct effects on sunlight absorbance, the heterotrophic

193 activity (including viral lysis) will increase local temperatures. Together, these effects may
194 significantly increase ice and snow melting in the Barents Sea region that is already one of the
195 fastest-warming regions on earth. Projections for global red snow coverage and its influence on
196 warming patterns should be investigated further.

197

198 **Acknowledgements**

199 Permitting for this work was from the Russian Federation (Ministry of Education and Research
200 #71; June 3, 2013). The authors are grateful to Alexander Chichaev, Roman Seliverstov, Pavel
201 Terekhov, Andrew Terekhov, and Sergey Kononov for keeping us alive above water and Dave
202 McAloney for underwater operations. The authors also thank Yuri Gavrilov (INTAARI,
203 St.Petersburg, Russia) and Paul Rose (Royal Geographic Society) for logistical help, as well as
204 the captain and crew of the M/V Polaris.
205

206

207 **References**

208

209 Bardgett RD, Freeman C, and Ostle NJ. 2008. Microbial contributions to climate change through
210 carbon cycle feedbacks. *Isme Journal* 2:805-814. DOI 10.1038/ismej.2008.58

211 Clarke AD, and Noone KJ. 1985. Soot in the Arctic Snowpack - a Cause for Perturbations in
212 Radiative-Transfer. *Atmospheric Environment* 19:2045-2053. Doi 10.1016/0004-
213 6981(85)90113-1

214 Dixon P. 2003. VEGAN, a package of R functions for community ecology. *Journal of*
215 *Vegetation Science* 14:927-930. DOI 10.1111/j.1654-1103.2003.tb02228.x

216 Geller A. 1986. Comparison of Mechanisms Enhancing Biodegradability of Refractory Lake
217 Water Constituents. *Limnology and Oceanography* 31:755-764.

218 Gorton HL, and Vogelmann TC. 2003. Ultraviolet radiation and the snow alga *Chlamydomonas*
219 *nivalis* (Bauer) Wille. *Photochemistry and Photobiology* 77:608-615. Doi 10.1562/0031-
220 8655(2003)077<0608:Uratsa>2.0.Co;2

221 Gradinger R, and Nurnberg D. 1996. Snow algal communities on Arctic pack ice floes
222 dominated by *Chlamydomonas nivalis* (Bauer) Wille. *Proceedings of the National Institute of*
223 *Polar Research Symposium on Polar Biology* 9:35-43.

224 Guiry MD, Guiry GM, Morrison L, Rindi F, Valenzuela Miranda S, Mathieson AC, Parker BC,
225 Langangen A, John DM, Barbara I, Carter CF, Kuipers P, and Garbary DJ. 2014. AlgaeBase:
226 an on-line resource for Algae. *Cryptogamie Algologie* 35:105-115. DOI
227 10.7872/crya.v35.iss2.2014.105

228 Hamer U, and Marschner B. 2002. Priming effects of sugars, amino acids, organic acids and
229 catechol on the mineralization of lignin and peat. *Journal of Plant Nutrition and Soil Science-*
230 *Zeitschrift Fur Pflanzenernahrung Und Bodenkunde* 165:261-268. Unsp [P88/4b]
231 Doi 10.1002/1522-2624(200206)165:3<261::Aid-Jpln261>3.0.Co;2-I

232 Kohshima S, Seko K, and Yoshimura Y. 1993. Biotic Acceleration of Glacier Melting in Yala
233 Glacier, Langtang Region, Nepal Himalaya. *Snow and Glacier Hydrology*:309-316.

234 Lutz S, Anesio AM, Villar SEJ, and Benning LG. 2014. Variations of algal communities cause
235 darkening of a Greenland glacier. *Fems Microbiology Ecology* 89:402-414. Doi
236 10.1111/1574-6941.12351

237 Maccario L, Vogel TM, and Larose C. 2014. Potential drivers of microbial community structure
238 and function in Arctic spring snow. *Frontiers in Microbiology* 5. ARTN 413
239 DOI 10.3389/fmicb.2014.00413

240 Madigan MT, Martinko JM, and Parker J. 1997. *Brock Biology of Microorganisms*: Prentice-
241 Hall, Upper Saddle River, NJ.

- 242 Muller T, Bleiss W, Martin CD, Rogaschewski S, and Fuhr G. 1998. Snow algae from northwest
243 Svalbard: their identification, distribution, pigment and nutrient content. *Polar Biology* 20:14-
244 32. DOI 10.1007/s003000050272
- 245 Remias D, Lutz-Meindl U, and Lutz C. 2005. Photosynthesis, pigments and ultrastructure of the
246 alpine snow alga *Chlamydomonas nivalis*. *European Journal of Phycology* 40:259-268. Doi
247 10.1080/09670260500202148
- 248 Rosen H, Novakov T, and Bodhaine BA. 1981. Soot in the Arctic. *Atmospheric Environment*
249 15:1371-1374. Doi 10.1016/0004-6981(81)90343-7
- 250 Schmieder R, and Edwards R. 2011a. Fast Identification and Removal of Sequence
251 Contamination from Genomic and Metagenomic Datasets. *Plos One* 6. ARTN e17288
252 DOI 10.1371/journal.pone.0017288
- 253 Schmieder R, and Edwards R. 2011b. Quality control and preprocessing of metagenomic
254 datasets. *Bioinformatics* 27:863-864. DOI 10.1093/bioinformatics/btr026
- 255 Sibandze P, Mhangara P, Odindi J, and Kganyago M. 2014. A comparison of Normalised
256 Difference Snow Index (NDSI) and Normalized Difference Principal Component Snow Index
257 (NDPCSI) techniques in distinguishing snow from related land cover types. . *South African*
258 *Journal of Geomatics* 3:197-209.
- 259 Stibal M, Elster J, Sabačka M, and Kastovská K. 2007. Seasonal and diel changes in
260 photosynthetic activity of the snow alga *Chlamydomonas nivalis* (Chlorophyceae) from
261 Svalbard determined by pulse amplitude modulation fluorometry. *Fems Microbiology*
262 *Ecology* 59:265-273. DOI 10.1111/j.1574-6941.2006.00264.x
- 263 Takeuchi N. 2009. Temporal and spatial variations in spectral reflectance and characteristics of
264 surface dust on Gulkana Glacier, Alaska Range. *Journal of Glaciology* 55:701-709.
- 265 Takeuchi N, Dial R, Kohshima S, Segawa T, and Uetake J. 2006. Spatial distribution and
266 abundance of red snow algae on the Harding Icefield, Alaska derived from a satellite image.
267 *Geophysical Research Letters* 33. Artn L21502
268 Doi 10.1029/2006gl027819
- 269 Thevenon F, Anselmetti FS, Bernasconi SM, and Schwikowski M. 2009. Mineral dust and
270 elemental black carbon records from an Alpine ice core (Colle Gnifetti glacier) over the last
271 millennium. *Journal of Geophysical Research-Atmospheres* 114. Artn D17102
272 10.1029/2008jd011490
- 273 Thomas WH, and Duval B. 1995. Sierra-Nevada, California, USA, Snow Algae - Snow Albedo
274 Changes, Algal Bacterial Interrelationships, and Ultraviolet-Radiation Effects. *Arctic and*
275 *Alpine Research* 27:389-399. Doi 10.2307/1552032
- 276 van Nugteren P, Moodley L, Brummer GJ, Heip CHR, Herman PMJ, and Middelburg JJ. 2009.
277 Seafloor ecosystem functioning: the importance of organic matter priming. *Marine Biology*
278 156:2277-2287. 10.1007/s00227-009-1255-5

279 Williams WE, Gorton HL, and Vogelmann TC. 2003. Surface gas-exchange processes of snow
280 algae. *Proceedings of the National Academy of Sciences of the United States of America*
281 100:562-566. DOI 10.1073/pnas.0235560100

282

283

284 **Figure Legends**

285

286 **Figure 1.** (A) A time series comparison of the percentage of total snow or ice that is covered
287 with algae at selected alpine and polar regions throughout the world, according to data derived
288 from satellite images. (B) A time series comparison of the total area of snow and sea ice, total
289 algal biomass, and percentage of total snow that is covered with algae within the map extent near
290 Nansen Island, Franz Josef Land, for years 1986, 2002, 2006 and 2015. The colored time series
291 shows spatial distribution maps of algal densities of the Nansen Island area in Franz Josef Land.

292

293 **Figure 2.** (A) Abundances of viruses, Bacteria and Eukaryotes in samples from red snow and
294 snow communities. The y-axis shows abundances after normalizing and standardizing raw read
295 counts to ensure cross-sample comparisons are valid. (B) Bar plots showing abundances of two
296 Eukaryotic phyla found in red snow and snow communities. Chlorophyta is the phylum that
297 contains the genus *Chlamydomonas*.

298

299 **Figure 3.** (A) Bar plots showing functional pathways that were statistically significantly
300 different in abundance between red snow and snow. (B) Bar plots depicting energy metabolism
301 pathways and their abundances in red snow and snow.

302

303 **Figure 4.** Model of *C. nivalis* in white and red snows. The left panel shows several microbial
304 communities that are found in white snow. Sunlight promotes astaxanthin expression in *C.*
305 *nivalis*, turning the snow to red and promoting community metabolism shifts through stimulation
306 of heterotrophic metabolism. The *C. nivalis* blooms, albedo is decreased and local snow and ice
307 melts at a faster rate (right panel).

308

309

Figure 1 (on next page)

Changes in red snow through time

(A) A time series comparison of the percentage of total snow or ice that is covered with algae at selected alpine and polar regions throughout the world, according to data derived from satellite images. (B) A time series comparison of the total area of snow and sea ice, total algal biomass, and percentage of total snow that is covered with algae within the map extent near Nansen Island, Franz Josef Land, for years 1986, 2002, 2006 and 2015. The colored time series shows spatial distribution maps of algal densities of the Nansen Island area in Franz Josef Land.

A



B

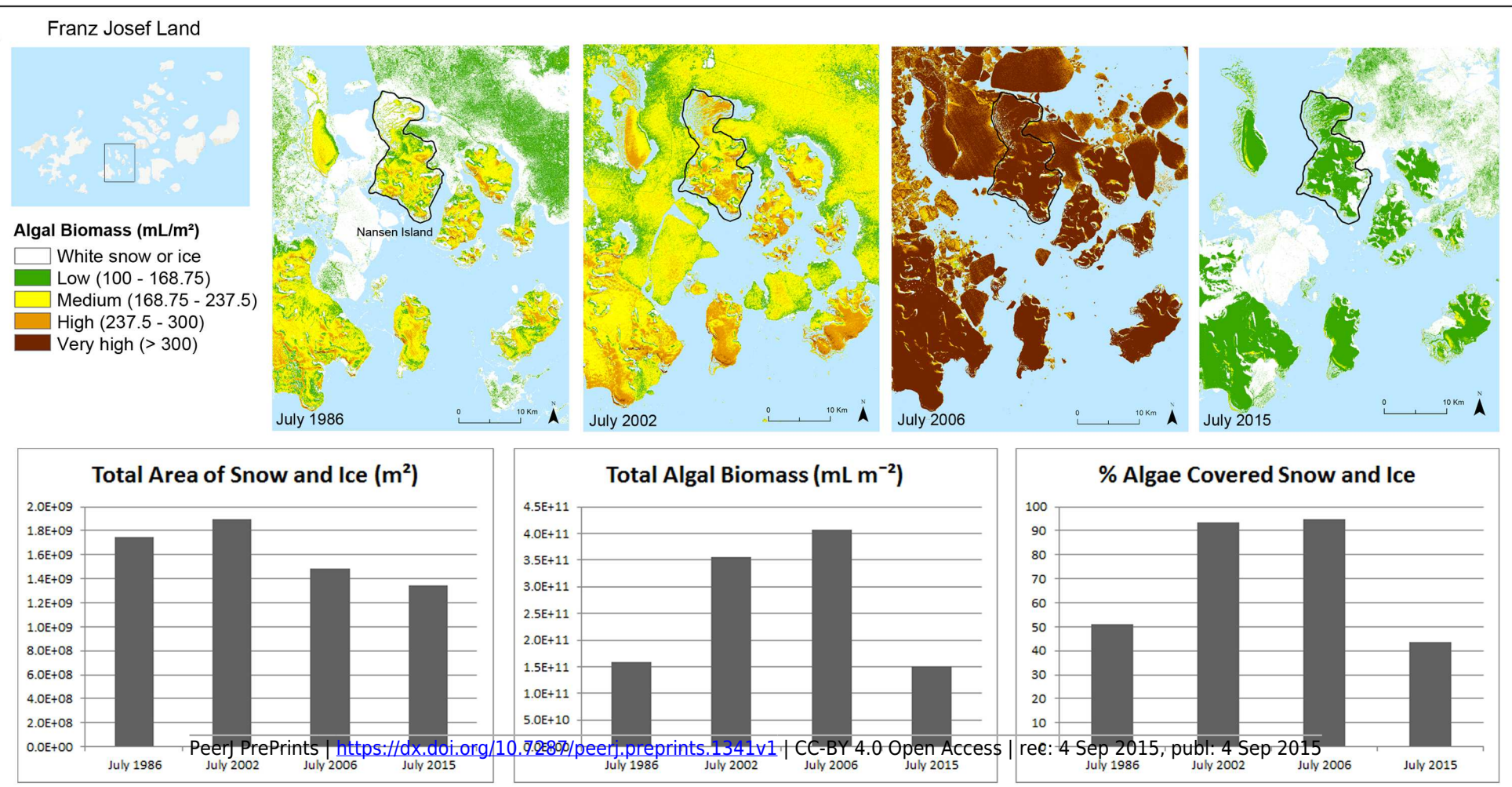


Figure 2 (on next page)

Abundances of microbes in red snow and white snow samples

(A) Abundances of viruses, Bacteria and Eukaryotes in samples from red snow and snow communities. The y-axis shows abundances after normalizing and standardizing raw read counts to ensure cross-sample comparisons are valid. (B) Bar plots showing abundances of two Eukaryotic phyla found in red snow and snow communities. Chlorophyta is the phylum that contains the genus *Chlamydomonas*.

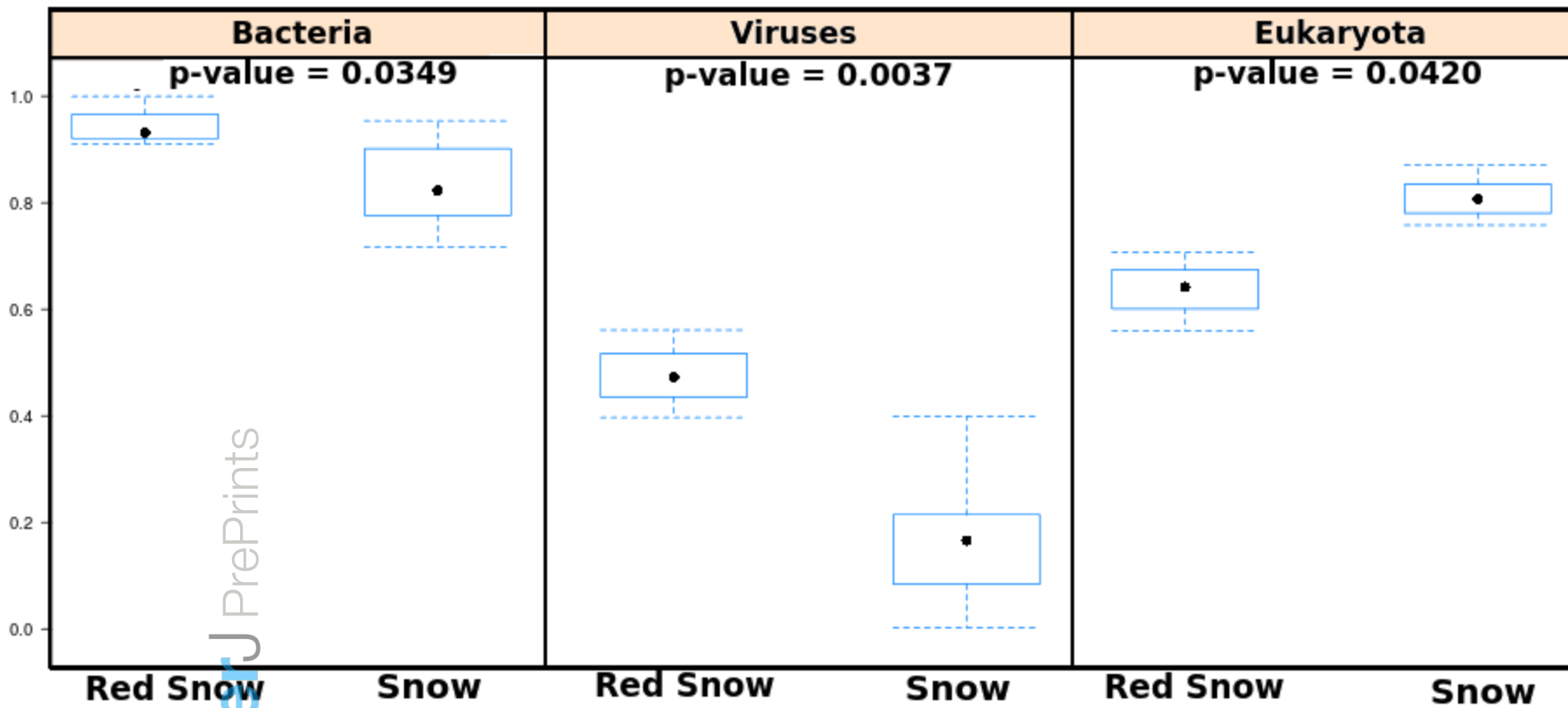
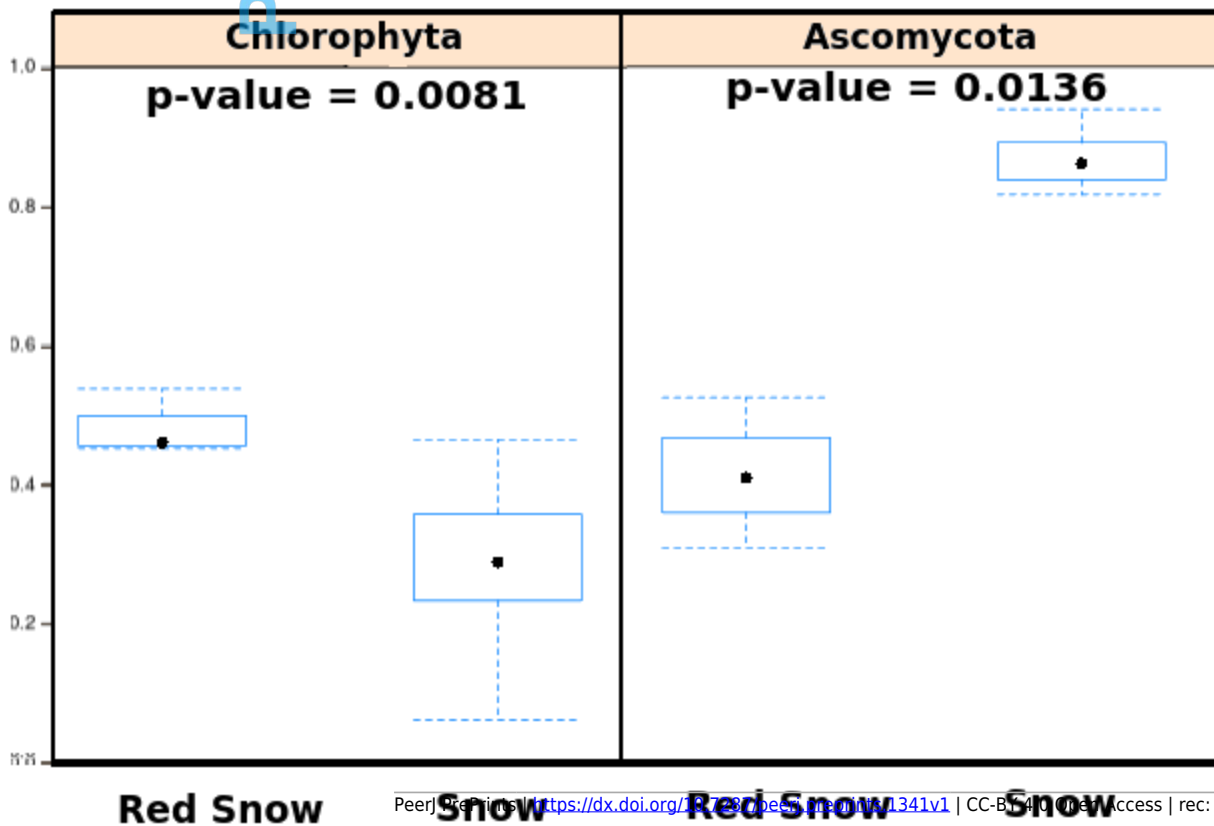
A**B**

Figure 3(on next page)

Functional pathways in red snow and white snow

(A) Bar plots showing functional pathways that were statistically significantly different in abundance between red snow and snow. (B) Bar plots depicting energy metabolism pathways and their abundances in red snow and snow.

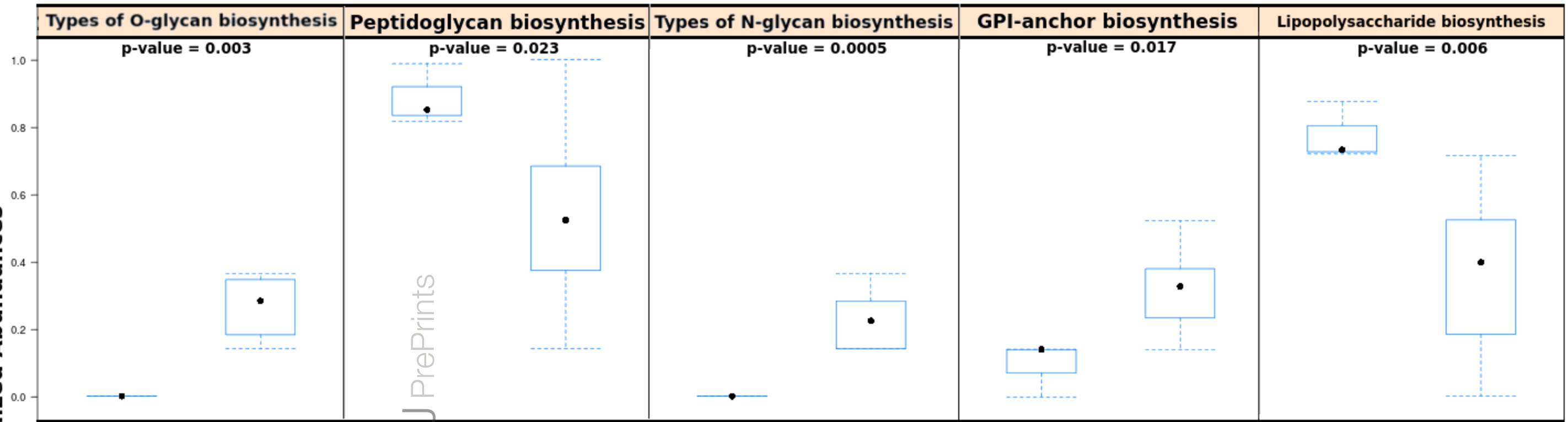
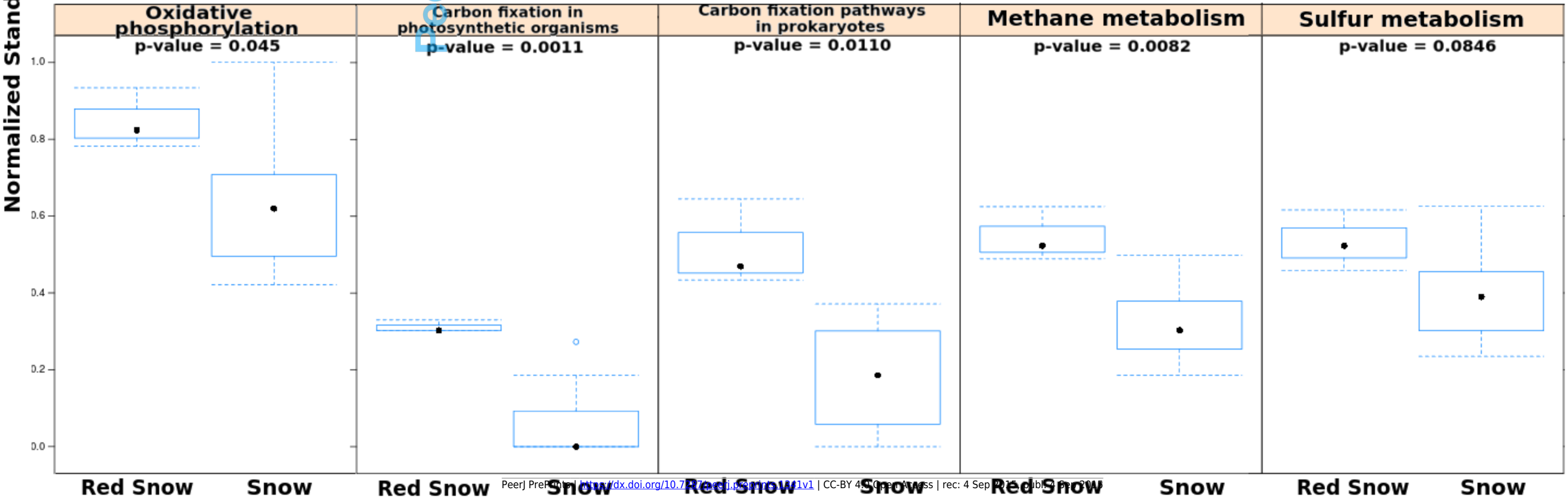
A**B**

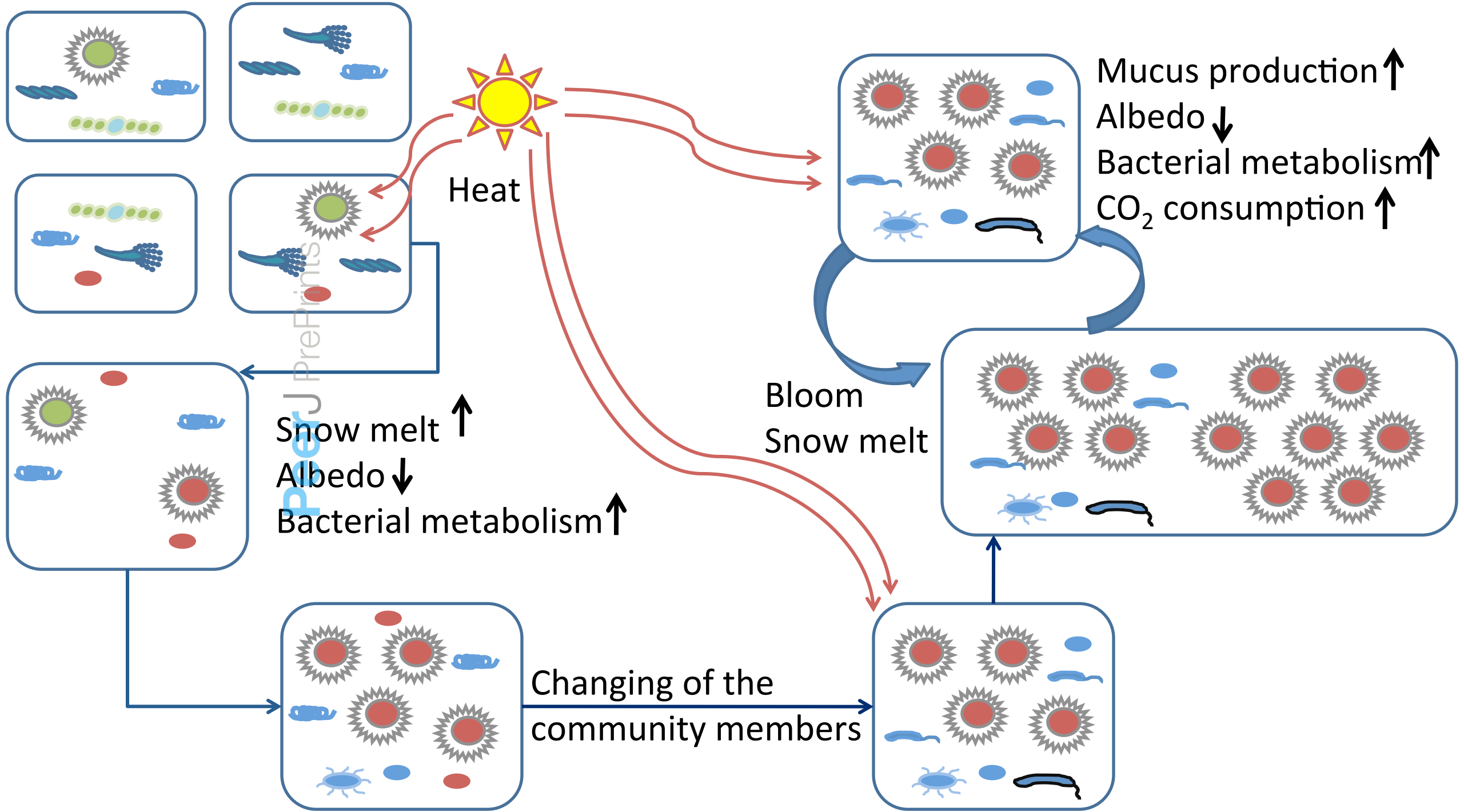
Figure 4 (on next page)


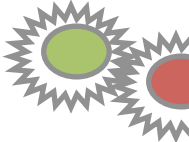








Model of red snow microbiology

Model of *C. nivalis* in white and red snows. The left panel shows several microbial communities that are found in white snow. Sunlight promotes astaxanthin expression in *C. nivalis*, turning the snow to red and promoting community metabolism shifts through stimulation of heterotrophic metabolism. The *C. nivalis* blooms, albedo is decreased and local snow and ice melts at a faster rate (right panel).

SNOW

RED SNOW



-  *Aspergillus*
-  *C. nivalis*
-  *Bacillus*
-  *Alteromonas*
-  *Neurospora*
-  *Nostoc*
-  *Pedobacter*
-  *Vibrio*
-  *Pseudoalteromonas*
-  *Spirosoma*